Geophysical Research Letters

RESEARCH LETTER
10.1029/2019GL083720

Key Points:
- New field data show water surface slopes vary significantly at a major planform transition, but minimally elsewhere
- Spatial coverage of existing satellite altimetry may be adequate for Congo River water slopes in the Cuvette Centrale, but not the outlet
- Adjustment of depth is the main mechanism for conserving mass at width constrictions, minimizing variability in water slope and velocity

Supporting Information:
- Supporting Information S1

Correspondence to:
A. B. Carr,
cen4abc@leeds.ac.uk

Citation:
Carr, A. B., Trigg, M. A., Tshimanga, R. M., Borman, D. J., & Smith, M. W. (2019). Greater water surface variability revealed by new Congo River field data: Implications for satellite altimetry measurements of large rivers. *Geophysical Research Letters*, *46*, 8093–8101. https://doi.org/10.1029/2019GL083720

Received 17 MAY 2019
Accepted 29 JUN 2019
Accepted article online 8 JUL 2019
Published online 17 JUL 2019

Greater Water Surface Variability Revealed by New Congo River Field Data: Implications for Satellite Altimetry Measurements of Large Rivers

Andrew B. Carr[1], Mark A. Trigg[1], Raphael M. Tshimanga[2,3], Duncan J. Borman[1], and Mark W. Smith[4]

[1]School of Civil Engineering, University of Leeds, Leeds, UK, [2]Department of Natural Resources Management, University of Kinshasa, Kinshasa, DR, Congo, [3]Congo Basin Water Resources Research Center (CRREBaC), University of Kinshasa, Kinshasa, DR, Congo, [4]School of Geography, University of Leeds, Leeds, UK

Abstract Large river hydrodynamics studies inform global and regional issues pertaining to biogeochemical cycling, ecology, water availability, and flood risk. Such studies rely increasingly on satellite measurements, but these are limited by resolution, coverage, and uncertainty and their inability to directly measure bathymetry or discharge. We obtain new in situ data covering 650 km of the Congo's main stem, including elusive bathymetry and discharge measurements that complement space-borne data sets. Our key findings relate to our water surface elevation measurements, which show that spatial coverage of existing satellite altimetry for deriving river water surface profiles may be adequate through the globally important Cuvette Centrale but is not at its outlet where our field data reveal significant spatial variability in water surface slope. The findings have implications for altimetry-based hydrodynamics studies of other large rivers, such as those that involve estimating discharge or modeling multichannel river hydraulics.

Plain Language Summary Understanding the dynamics of surface water along the world's large river channel systems is of major importance. For example, it controls the duration and extents of floods that sustain globally important floodplain and wetland ecosystems. However, this understanding remains poor for unmonitored systems where access is difficult. In this study, we report results from a field campaign covering 650 km of the Congo River. Key measurements of river depth, flow rate, velocity, and water surface elevation are combined with satellite measurements to characterize this system. We find flow conditions vary minimally along most of the 650 km surveyed. However, significant changes occur along a 150-km reach at the outlet of the Cuvette Centrale wetland region, and a comparison of different data sets shows that measurements of water surface elevation from space by satellites have insufficient coverage to detect major changes in the water surface at this location. These findings have important implications given the widespread use of these satellite measurements in a number of applications such as computer modeling of floods and the estimation of river flows from space.

1. Introduction

Satellite measurements are expected to play an increasingly important role in the study of river hydrodynamics globally, as they can provide consistent and near real time monitoring over large areas. Inland open water surface elevation (WSE) measurements derived from satellite altimeters are a primary component of many satellite remote sensing (SRS) studies of large river hydrodynamics. In remote regions lacking in situ data, these studies are valuable for understanding flood risk, water availability, and for global biogeochemical and ecological processes, because of the role large river floodplains and wetlands play in global fluxes of methane and CO_2 (Richey et al., 2002). Key applications relevant to this study include characterizing river hydrodynamics (e.g., (Birkett et al., 2002)) and calibration and validation of hydraulic river models (e.g., (Neal et al., 2012)). Moreover, estimation of discharge at ungauged river reaches combines altimetry estimates of WSE and water surface slope (WSS) with satellite imagery estimates of river width and minimal in situ observations (Birkinshaw et al., 2014; Bjerklie et al., 2018).

A growing number of radar and laser satellite altimeters have measured WSE with an accuracy of 0.35 m or less (Frappart et al., 2006; Jarihani et al., 2013; Urban et al., 2008) and are therefore considered suitable for SRS river hydrodynamics studies (Domeneghetti et al., 2015). However, use of altimetry data in a river hydrodynamics context is limited by data coverage in both time and space, which may be insufficient to capture key spatiotemporal variations in WSE and WSS. Such variations are important for characterizing the hydraulic behavior of river reaches (de Moraes et al., 2017; Garambois et al., 2016; Montazem et al., 2019). Field campaigns can obtain data with denser or more consistent coverage, and target particular locations in space and time. Bathymetry and discharge can also be obtained; such measurements cannot be obtained directly from SRS but are key parameters in river hydrodynamics. Field data and SRS are therefore complementary, because when combined, they provide comprehensive hydraulic data sets. Moreover, field data can be used to validate SRS measurements and determine the capabilities of valuable SRS data sets that cover far greater temporal and spatial extents.

The aim of this study is to review newly acquired hydraulic field data for one of the world's largest but least studied rivers, the Congo River. We identify new hydraulic characteristics of the Congo and investigate the value of SRS in studying large river hydrodynamics by comparing altimetry and in situ measurements. Specifically, we explore the spatial adequacy of altimetry for estimating WSE and WSS. The Congo River is an appropriate study area because of its status as a global hydrological research priority (Alsdorf et al., 2016) and one of the world's foremost candidates for SRS, due to lack of in situ data, access, and scale.

2. Study Area

The Congo River ranks second globally by discharge, with a mean annual discharge of 40,600 m^3/s (Laraque et al., 2001). The 1,700-km-long middle reach between Kinshasa and Kisangani (Figure 1) is an important resource for Central Africa, particularly for inland navigation. A network of 17,000 km of navigable river channels serves as the main mode of transport in the region (CICOS, 2015). The Congo's middle reach flows through the Cuvette Centrale wetland region, which functions as a globally significant source and sink of carbon; it contains the world's largest tropical peatland, which combined with above ground flooded forests are estimated to contain 35 petagrams of carbon (Dargie et al., 2017). Flooding in the Cuvette Centrale is clearly important for sustaining these wetlands and peatlands but also produces an estimated 0.4 petagrams of carbon per year at present from outgassing of carbon dioxide and methane (Borges et al., 2015; Bwangoy et al., 2010). Knowledge of main stem channel hydraulics is relevant to these carbon and methane fluxes because it is required to simulate flood inundation dynamics, which can improve estimates of flood extent and duration and hence outgassing estimates, and give insights into how susceptible wetlands are to future hydrological variability caused by potential climate and land use changes.

In situ data for the Congo are severely lacking due to a major decline in gauging infrastructure (Croneborg, 2013; Tshimanga & Hughes, 2014) and limited access due to a lack of infrastructure. This has led to an increasing reliance on SRS to study the hydrology and hydrodynamics of the Congo, particularly the middle reach. Here, the river is highly subcritical and has very gradually variable flow conditions in both time and space due to its large size, mild bed slopes, and absence of falls or rapids (Robert, 1946). These characteristics are advantageous for the use of SRS data sets given their limited coverage. However, SRS data sets are limited by the extensive dense forestry that covers much of the Congo Basin, which makes inundation extents difficult to observe and topographic data subject to large uncertainties. WSE measurements of open water from satellite altimetry are therefore of particular value.

3. Methods and Data Sets

3.1. Field Data

Our field campaign included a hydraulic and bathymetric survey of a 650-km study reach of the Congo River (Figure 1), traveling by boat exclusively. This reach includes a significant part of the Cuvette Centrale, including its outlet, and the Oubangui, Sangha, and Kasai confluences. The morphology of the river here is diverse, based on the large variations in river width and number of channels (O'Loughlin et al., 2013). Examples of this diverse morphology include the Malebo Pool located at a river chainage (defined as "river centreline distance") of 0–50 km upstream of Kinshasa and the narrow single channel section of river known as the Chenal at chainage 50–270 km. At chainage 270 km the river changes its planform significantly, becoming multichannel and often greater than 10 km wide. Three lateral constrictions exist at chainage 300, 480, and 550 km where effective river width reduces to less than half of the reach average. To the

10.1029/2019GL083720

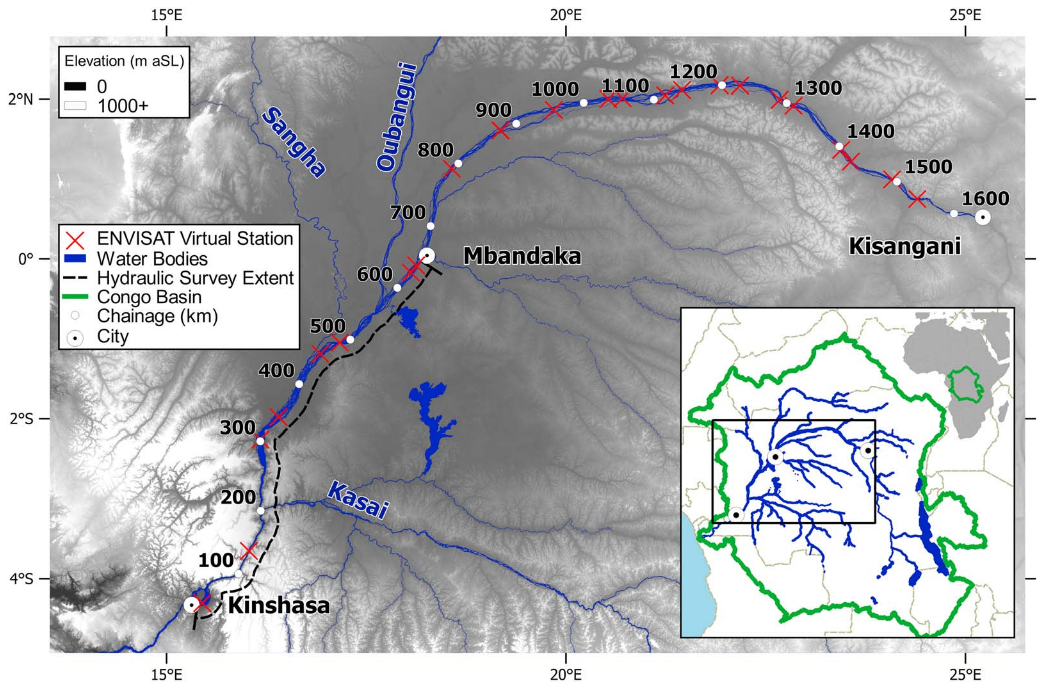

Figure 1. Map showing hydraulic survey extent and main stem ENVISAT Virtual Station locations (Santos da Silva et al., 2010). "Chainage" is river distance measured upstream of Kinshasa. Malebo Pool is situated at chainage 0–50 km, The Chenal runs from chainage 50–270 km. Three lateral constrictions in river width are located at chainage 300, 480, and 550 km. Elevations are from MERIT (Yamazaki et al., 2017); water bodies are from LANDSAT (CARPE, 2017; O'Loughlin et al., 2013).

authors' knowledge, the data obtained represents the first in situ hydraulic data set for the Congo River's middle reach available for scientific purposes since the establishment of modern hydrographic instruments such as acoustic Doppler current profilers (ADCPs).

The survey was conducted between 28 July and 16 August 2017, representing low-flow season for the main stem and the Kasai River, with the Oubangui River typically halfway up its rising limb (Becker et al., 2014). We collected WSE data along this reach at a maximum interval of 100 km using a Trimble R10 Global Navigation Satellite System (GNSS). These measurements were made at river shorelines using a live satellite correction service, which reports a vertical accuracy of 5-cm root mean square (RMS) error (Trimble, 2019). Measurement precision was checked by measuring an historic benchmark at chainage 160 km over 3 days, which gave a standard deviation of 3.4 cm. Multiple measurements were also taken at each shoreline WSE location; the maximum standard deviation of these was 6.4 cm at chainage 160 km.

ADCP transects were taken at eight locations using a Teledyne RiverRay, to obtain discharge, velocity, and cross-sectional bathymetry. Transect resolution varied, with a mean bin size of 1.4 m and maximum bin size of 2 m. Measurement precision was checked with transect repeatability tests, which showed a maximum discharge measurement variability of 2% at chainage 515 km. Accuracy was verified by a measurement near Kinshasa, which was within 1% of the value recorded by an in situ gauge at Kinshasa (IRD, 2019). River depth was measured continuously between Kinshasa and Mbandaka using a Garmin GT22 single beam echo sounder, with a spatial coverage of approximately 2 m in the direction of travel. Interrogation of all crossover points where depth was measured twice within 5 m horizontally gave a standard deviation of 0.34 m or 8%. The sonar measurement sequence was predominantly stream wise in orientation (i.e., not cross-sectional), it not being feasible to regularly sample the entire cross-section due to the many large islands that prevent bank-to-bank movement. Within the multichannel reaches, our sonar measurements sample the deeper channel threads; this is due to the boat captain's strict adherence to a navigation route established around 100 years ago, which is designed to minimize high-risk shallow water zones by following the deeper channel threads.

3.2. Satellite Altimetry

We use altimetry data to produce longitudinal plots of WSE in order to analyze spatial variability in WSS along the entire middle reach. Two periods are considered, July–August representing low flow and corresponding to our field campaign and December–January representing high flow. We primarily use ENVISAT, the most widely used source of WSE in the Congo Basin: Relevant examples of its use include studies of wetland inundation dynamics and river/floodplain interactions (Lee et al., 2011) and estimation of discharge from space (Kim et al., 2019). The widespread use of ENVISAT is due to its comparatively high spatiotemporal coverage and long temporal record—there are 23 overpasses, known as "virtual stations" (VSs), available through the middle reach (Figure 1), that were operational from 2002 to 2010. Each VS has an average temporal coverage of 10 measurements per year. ENVISAT accuracy for sufficiently wide rivers (~1 km wide) has been shown to be <0.3 m (Frappart et al., 2006). We also use data from the Sentinel-3A satellite that became operational in 2016. There is less than 3 years of data at the time of writing, and performance evaluation is limited, although a recent study on the Niger River reported improved performance of Sentinel-3A compared with well-established altimeters including ENVISAT (Normandin et al., 2018). However, it was operational during our field campaign so is of use for comparative purposes. We obtain ENVISAT and Sentinel-3A data sets from the Hydroweb database (Santos da Silva et al., 2010). We also use published ICESAT data (O'Loughlin et al., 2016; Zwally et al., 2012) for comparative purposes, although its use is limited in this study because ICESAT data are unavailable during July, August, or January and its lack of repeat passes produced only single measurements in time.

4. Results

4.1. Middle Reach WSE From Satellite Altimetry

We examine middle reach water surface profiles (WSPs) that are representative of seasonal low and high flow by plotting the mean average of all WSEs recorded during July and August, and December and January (low flow and high flow, respectively) at each ENVISAT VS. We also plot WSS calculated for each pair of WSEs and show effective river width derived from Landsat imagery (O'Loughlin et al., 2013). These are shown in Figure 2.

We find that 1,200 km of the middle reach WSE from Kinshasa to approximately the upstream maximum extent of the Cuvette Centrale is well represented by a second-order polynomial regression, describing a gradual flattening of the slope in the downstream direction. For low-flow WSEs, maximum regression residual is 0.36 m, and RMS is 0.19 m. For high-flow WSEs, maximum regression residual is 0.26 m, and RMS is 0.15 m. From 1,200 to 1,600 km the WSS becomes more variable. Based on a separate second-order polynomial, maximum regression residual for low flows is 0.55 m, and RMS is 0.30 m, and for high-flow WSEs, maximum regression residual is 0.36 m, and RMS is 0.24 m.

4.2. Hydraulic Survey

Results of WSE, discharge, velocity, and bathymetry measurements along the study reach (Carr et al., 2019) are plotted longitudinally (Figure 3). A GNSS WSP is shown by linearly interpolating the GNSS WSEs. We verified this linear interpolation by obtaining higher-resolution WSE data at chainage 270–310 km; a resulting 5-km resolution WSP plot is contained in Figure S1 in the supporting information. Measured bathymetric depths were converted to elevations by subtracting the depths from the GNSS WSP. By averaging the bathymetry measurements over a 5-km interval (typical river width) and a larger 50-km interval (reach scale), we remove localized variability and enable better interpretation of bed slopes and river depths at this scale. Standard deviations of the 5-km intervals express the variability across each interval.

Between 300 and 650 km is the multichannel part of the study reach located in the Cuvette Centrale. Here, the in situ WSE behavior is as shown by ENVISAT. WSS is highly regular, most notably through chainage 480–610 km where there are four GNSS measurements, and the river goes through two major width constrictions and the Oubangui confluence. The bathymetry clearly responds to river width by deepening at constrictions. Bed slope is relatively constant and almost parallel to the WSE at the 50-km scale, implying close to normal depth conditions. Average river depths also remain relatively constant through the

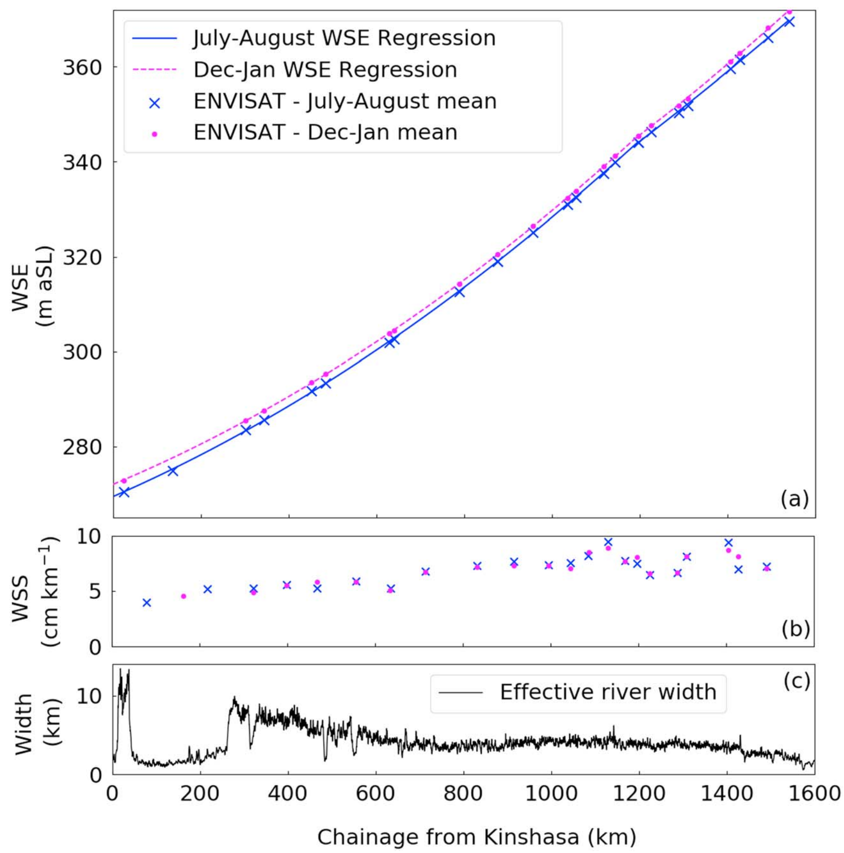

Figure 2. Longitudinal sections through the Congo middle reach main stem: (a) mean ENVISAT water surface elevations (WSEs) for July–August (low flow) and December–January (high flow), each with second-order polynomial curves fitted between chainage 0–1,200 km and 1,200–1,600 km; (b) low and high water surface slopes (WSS) calculated for each pair of mean WSEs; (c) effective river width derived from Landsat Imagery (O'Loughlin et al., 2013).

Oubangui confluence. Measured mean cross-sectional velocities are in the range of 0.75–0.95 m/s, which is highly consistent. While most ADCP transects were taken at width constrictions, two transects were also made at a more typical river width to sample the velocity in a morphological setting more representative of the middle reach. One such transect at 515 km sampled the entire river channel; the other, at 525 km, sampled a single channel thread within a multichannel reach that conveyed approximately 50% of the river discharge. These two transects show no marked decrease in mean velocity. Moreover, of the small velocity variations that were observed, velocities at two of the constrictions are lower than the wide multichannel values, with only the chainage 485-km constriction velocity shown to be slightly higher than the multichannel values. This shows the width constrictions do not cause significant flow accelerations during low flows and that mass is conserved predominantly by a local increase in channel depth.

As the river planform changes at chainage 270 km, the WSS varies considerably as a result of major changes in bathymetry and the Kasai confluence. The WSS steepens to 8 cm/km as it approaches the entrance to the Chenal and causes especially shallow river depths here. The WSS flattens after entering the Chenal and reduces to only 2 cm/km at the Kasai confluence. The 50-km scale bed slope is variable and consistently differs from the WSS.

The significant change in hydraulics and specifically WSS at the entrance to the Chenal has not been noted before. Capturing such spatial variability in WSS is important for characterizing the hydraulic behavior of river reaches for a range of hydrodynamic purposes, including derivation of discharge, which is of interest here for monitoring wetland outflows. The physiography of the river in this location is also conducive to obtaining requisite measurements of river width during high flows, it being single

10.1029/2019GL083720

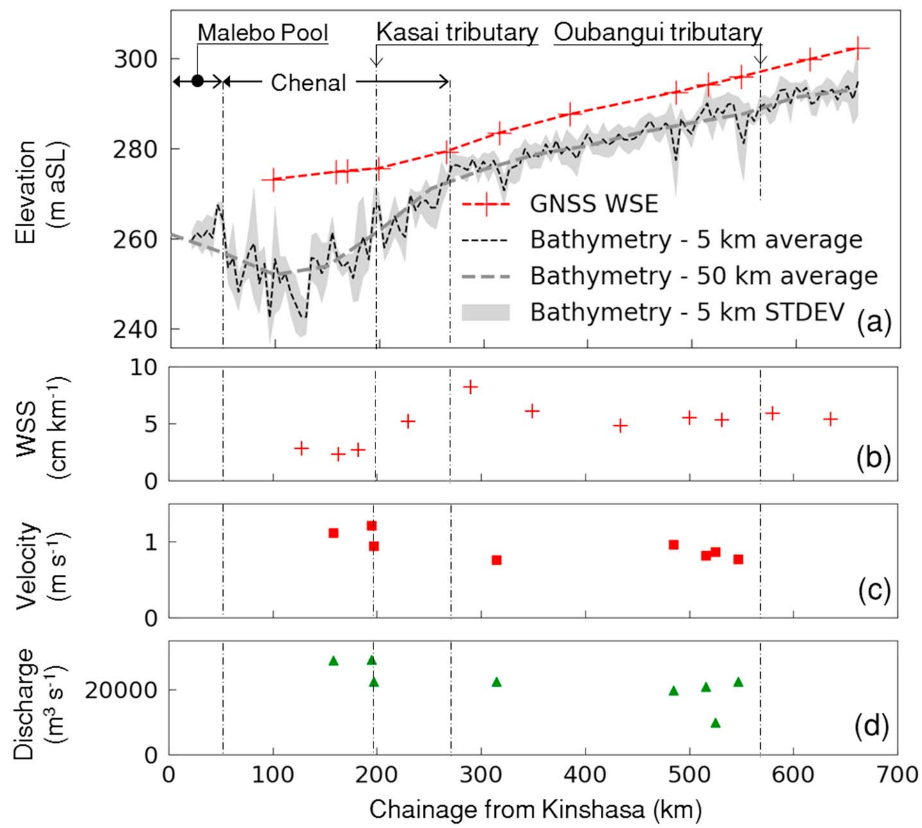

Figure 3. Key field campaign results plotted longitudinally: (a) water surface elevations (WSEs) measured with Global Navigation Satellite System (GNSS), Longitudinal Bathymetry measured with sonar and averaged over 5- and 50-km intervals; (b) water surface slope (WSS) calculated from each WSE pair; (c) acoustic Doppler current profiler measured cross-sectional average velocities; (d) acoustic Doppler current profiler measured discharge (including individual channel thread measurement at chainage 525 km). STDEV = Standard deviation.

channel, lacking extensive vegetated floodplains, and having relatively stable planform morphology (Pekel et al., 2016).

4.3. Comparison of GNSS and Altimetry

To look more closely at the WSS variability, we plot the GNSS WSEs with a range of comparative altimetry data sets (Figure 4). The GNSS WSEs were consistently lower than the mean low-flow ENIVSAT WSEs plotted in Figure 2, leading us to use the minimum July–August ENVISAT WSE at each VS, which are more representative of conditions during the field campaign. Use of minima instead of mean had no noticeable effect on the resulting WSP—repeating the regression analysis for the ENVISAT minima gave a standard deviation of 0.25 m and max residual of 0.56 m for chainage 0–1,200 km. We also plot new Sentinel 3A data here because we can obtain comparable WSEs by temporally interpolating measurements made by the satellite around the field campaign period. June ICESAT measurements for three separate years are also shown. The plotted ENVISAT WSP is the second-order polynomial regression, whereas the GNSS WSP is obtained by piecewise linear interpolation.

The ENVISAT WSE and WSS closely match the GNSS from chainage 325–650 km, maximum deviation from the GNSS being 0.30 m at chainage 345 km. Through chainage 100–300 km the low-flow ENVISAT WSP overestimates WSE by up to 2 m due to insufficient spatial coverage and is equivalent to approximately half of the annual flood-wave amplitude defined by the ENVISAT low- and high-flow WSEs. These overestimates of WSE could propagate upstream in hydraulic models and affect inundation predictions through the Cuvette Centrale and along the Kasai. The overestimate would also locally affect estimation of discharge. By applying Manning's equation to the river reach between chainage 200–270 km, we can assess the WSE overestimate in discharge terms:

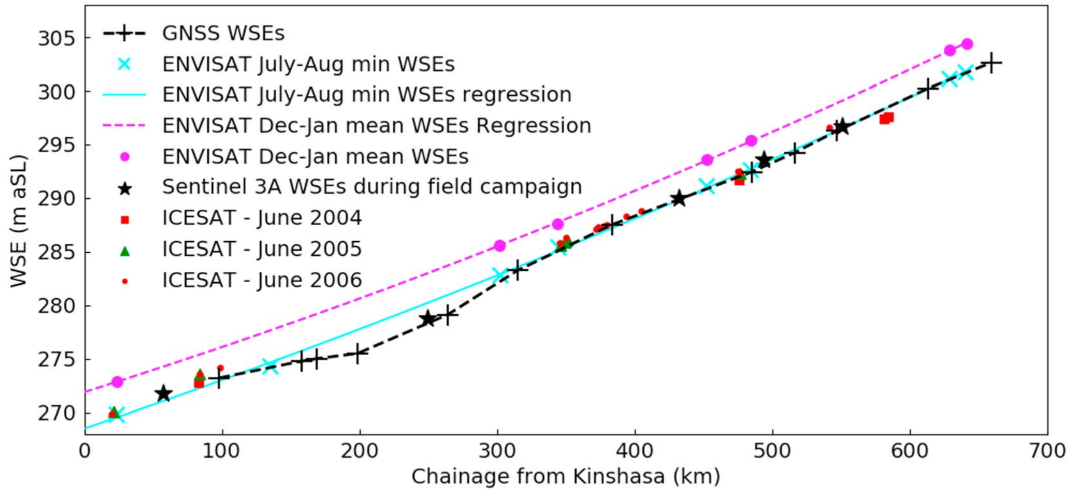

Figure 4. Plot of Global Navigation Satellite System (GNSS) water surface elevations (WSEs) and comparative low-flow altimetry WSEs from ENVISAT, Sentinel-3A, and ICESAT. High-flow (mean December and January) ENVISAT WSEs are also shown to convey the magnitude of flood-wave amplitude. GNSS WSEs are linearly interpolated piecewise. Sentinel 3A WSEs are linearly interpolated temporally to derive WSEs during field campaign.

$$Q = A\left({}^{1}/_{n}\right)m^{2/3}i^{1/2}, \tag{1}$$

where Q is discharge (m^3/s), A is cross-sectional area (m^2), n is Mannings hydraulic roughness coefficient ($s/m^{1/3}$), m is the hydraulic radius (m^2/m), and i is the WSS (m/m). By approximating flow conditions as being uniform and representing the channel with the ADCP cross-section measured upstream of the Kasai confluence, we back calculate n using values of Q and WSE obtained from the field campaign (Figure 3). We then recalculate Q using the calculated value of n, and values of i and WSE from ENVISAT. The result is a difference of 8,300 m^3/s or 37% from the measured flow of 22,400 m^3/s.

The Sentinel-3A altimeter provides measurements at different locations to ENVISAT. The temporally interpolated WSEs show reasonable agreement with the GNSS WSP, with a maximum deviation of 0.60 m, which is partially due to the use of linear interpolation between data points that are up to 3 months apart. Notably, Sentinel-3A obtains measurements at chainage 250 km and identifies that there is WSS variability at the Cuvette Centrale outlet. The data point is not able to describe the WSS but is sufficient to define the WSE and partly validates our GNSS measurements. ICESAT does not identify the WSS variability.

5. Discussion

The minimal change in WSS and velocity observed through the Cuvette Centrale is in part due to the river channel deepening in response to constrictions in river width and maintaining a relatively consistent cross-sectional area through mass-conserved reaches. As a result, a relatively coarse and simple physical representation of bathymetry coupled with a spatially uniform river channel friction may suffice in hydraulic models for simulating flood dynamics. This has been demonstrated in other large rivers such as the Amazon (Trigg et al., 2009) but is an important finding on a morphologically complex multichannel river where obtaining a full bathymetry data set is challenging.

The lack of WSE definition through the Chenal with satellite altimetry is surprising given the size of the Congo River and the range of altimeters that have measured the Congo's WSE. Such undetected spatial variations in WSS are likely to exist on other large rivers. However, the Surface Water and Ocean Topography (SWOT) mission will address this knowledge gap. SWOT's KaRIN interferometer will measure WSE with subkilometer spatial resolution at least once every 21 days (Biancamaria et al., 2016), providing more than sufficient WSE information for capturing WSS variability observed here. Outside of SWOT's 3-year operational lifetime, long or nonrepeat orbit altimeters can offer a denser spatial coverage or higher-accuracy WSE data than VS data. CryoSat-2 provides dense spatial coverage with an intertrack distance of 7.5 km at the equator (Schneider et al., 2018), and recently launched ICESAT-2 is expected to provide higher-accuracy WSE information that can validate measurements of WSE and WSS from other altimeters (Escobar et al., 2015). Such long or nonrepeat altimetry can be useful for parameterizing, calibrating, and validating hydraulic models and WSS, particularly where the spatial coverage of VS is inadequate. However, their low temporal resolution limits their use for generating WSPs and estimating WSS.

The data and analysis presented in this paper are the first key steps in understanding this river, and enabling the development of hydraulically correct river models for this, and potentially other similarly large morphologically complex systems. Further progress toward this may be achieved through numerical hydraulic modeling experiments used to identify effective representations of large multichannel river bathymetry in such models. This work also presents opportunities for testing the ability of discharge estimation algorithms to translate SWOT WSE measurements into discharge in large multichannel rivers; the in situ hydraulic data presented here may serve as a priori information and validation data.

6. Conclusions

We have conducted the first hydraulic research field campaign in recent decades for the middle reach of the Congo River, which has provided a rare opportunity to study the hydraulics of a large, complex planform system. We find the majority of a 650-km study reach is characterized by only very gradual spatial changes in WSS (5–6 cm/km) and velocity (0.75–0.95 m/s) during low flows, neither of which are affected by changes in bathymetry despite its highly diverse and multichannel nature. These results show that a relatively coarse and simple physical representation of river bathymetry may be sufficient for use in hydraulic models used to simulate hydrodynamics here, and potentially along reaches of other large multichannel rivers.

However, this characterization does not hold for a 150-km reach located at the outlet of the Cuvette Centrale, where changes in bathymetry and the presence of a large tributary cause WSS to vary spatially from 2 to 8 cm/km. Current altimetry data sets perform poorly at estimating WSE and WSS in this reach; an ENVISAT-derived WSP deviates from field measurements by up to 2 m due to insufficient spatial resolution, which represents approximately half the annual flood-wave amplitude, or a 37% difference when used to compute discharge. These findings are unexpected for a reach of the world's second largest river that is hydraulically subcritical and shows SWOT's high-resolution measurements are needed to sufficiently remotely capture WSS variability on even the world's largest rivers.

Acknowledgments
The field campaign was conducted by the Congo River user Hydraulics and Morphology (CRuHM) project, which is wholly funded by The Royal Society-DFID Africa Capacity Building Initiative (RS-DFID Grant AQ150005). The authors would like to acknowledge the CRuHM 2017 fieldwork team and la Régie des voies fluviales (RVF) in DR Congo for their logistical and technical support during the field campaign. A. B. C. is funded by a Leeds Anniversary Research Scholarship. The processed data from this field campaign used in this paper can be obtained from a HYDROSHARE repository (https://doi.org/10.4211/hs.e5da4bdf5b474b5bb9720387fed458ba). The ENVISAT and Sentinel-3A altimeter products were produced by Hydroweb and distributed by Theia, with support from Cnes and Legos (available at http://hydroweb.theia-land.fr/). We would like to thank Editor Valeriy Ivanov and two anonymous reviewers who provided constructive comments that helped improve the quality of the manuscript.

References

Alsdorf, D., Beighley, E., Laraque, A., Lee, H., Tshimanga, R., O'Loughlin, F., et al. (2016). Opportunities for hydrologic research in the Congo Basin. *Reviews of Geophysics*, *54*, 378–409. https://doi.org/10.1002/2016RG000517

Becker, M., Santos da Silva, J., Calmant, S., Robinet, V., Linguet, L., & Seyler, F. (2014). Water level fluctuations in the Congo Basin derived from ENVISAT satellite altimetry. *Remote Sensing*, *6*, 9340–9358. https://doi.org/10.3390/RS6109340

Biancamaria, S., Lettenmaier, D. P., & Pavelsky, T. M. (2016). The SWOT mission and its capabilities for land hydrology. *Surveys in Geophysics*, *37*(2), 307–337. https://doi.org/10.1007/s10712-015-9346-y

Birkett, C. M., Mertes, L. A. K., Dunne, T., Costa, M. H., & Jasinski, M. J. (2002). Surface water dynamics in the Amazon Basin: Application of satellite radar altimetry. *Journal of Geophysical Research*, *107*(D20), 8059. https://doi.org/10.1029/2001JD000609

Birkinshaw, S. J., Moore, P., Kilsby, C. G., Donnell, G. M. O., Hardy, A. J., & Berry, P. A. M. (2014). Daily discharge estimation at ungauged river sites using remote sensing. *Hydrological Processes*, *28*(3), 1043–1054. https://doi.org/10.1002/hyp.9647

Bjerklie, D. M., Birkett, C. M., Jones, J. W., Carabajal, C., Rover, J. A., Fulton, J. W., & Garambois, P. (2018). Satellite remote sensing estimation of river discharge: Application to the Yukon River Alaska. *Journal of Hydrology*, *561*(February), 1000–1018. https://doi.org/10.1016/j.jhydrol.2018.04.005

Borges, A. V., Darchambeau, F., Teodoru, C. R., Marwick, T. R., Tamooh, F., Geeraert, N., et al. (2015). Globally significant greenhouse-gas emissions from African inland waters. *Nature Geoscience*, *8*(8), 637–642. https://doi.org/10.1038/NGEO2486

Bwangoy, J. R. B., Hansen, M. C., Roy, D. P., de Grandi, G., & Justice, C. O. (2010). Wetland mapping in the Congo Basin using optical and radar remotely sensed data and derived topographical indices. *Remote Sensing of Environment*, *114*(1), 73–86. https://doi.org/10.1016/j.rse.2009.08.004

CARPE. (2017). Forest Atlas of DRC: Hydrographic network of the Democratic Republic of Congo. Retrieved December 5, 2017, from https://carpe-worldresources.opendata.arcgis.com/datasets/medd::streams?geometry=15.835%2C-1.698%2C17.57%2C-1.217

Carr, A. B., Trigg, M. A., Tshimanga, R. M., & Congo River users Hydraulics and Morphology Consortium. (2019). CRuHM 2017 Congo River Main Stem Processed Field Data: WSE, Bathymetry and Discharge, Hydroshare. https://doi.org/10.4211/hs.e5da4bdf5b474b5bb9720387fed458ba

CICOS. (2015). VOIES NAVIGABLES. Retrieved March 18, 2019, from http://www.cicos.int/navigation-interieure/voies-navigables/

Croneborg, L. E. M. (2013). Project information document (concept stage)—Strengthening hydro-meteorological and climate services in DRC - P144712 (English). Washington, D.C. : World Bank Group. Retrieved from http://documents.worldbank.org/curated/en/771081468230086348/Project-Information-Document-Concept-Stage-Strengthening-Hydro-Meteorological-and-Climate-Services-in-DRC-P144712

Dargie, G. C., Lewis, S. L., Lawson, I. T., Mitchard, E. T. A., Page, S. E., Bocko, Y. E., & Ifo, S. A. (2017). Age, extent and carbon storage of the central Congo Basin peatland complex. *Nature*, *542*(7639), 86–90. https://doi.org/10.1038/nature21048

Domeneghetti, A., Castellarin, A., Tarpanelli, A., & Moramarco, T. (2015). Investigating the uncertainty of satellite altimetry products for hydrodynamic modelling. *Hydrological Processes*, *29*(23), 4908–4918. https://doi.org/10.1002/hyp.10507

Escobar, V., Delgado Arias, S., Woo, L., Neumann, T., Jasinski, M., Brown, M., & Turner, W. (2015). Ice, cloud and land elevation Satellite-2 2nd applications workshop. Retrieved June 14, 2019, from https://icesat-2.gsfc.nasa.gov/sites/default/files/general_content_files/ICESat2_2ndApplicationsWorkshop_Report_Final_05August2015_0.pdf

Frappart, F., Calmant, S., Cauhopé, M., Seyler, F., & Cazenave, A. (2006). Preliminary results of ENVISAT RA-2-derived water levels validation over the Amazon basin. *Remote Sensing of Environment*, *100*(2), 252–264. https://doi.org/10.1016/j.rse.2005.10.027

Frasson, R. P. M., Wei, R., Durand, M., Minear, J. T., Domeneghetti, A., Schumann, G., Williams, B. A., et al. (2017). Automated river reach definition strategies: Applications for the surface water and ocean topography mission. *Water Resources Research*, *53*, 8164–8186. https://doi.org/10.1002/2017WR020887

Garambois, P. A., Calmant, S., Roux, H., Paris, A., Monnier, J., Finaud-Guyot, P., et al. (2016). Hydraulic visibility: Using satellite altimetry to parameterize a hydraulic model of an ungauged reach of a braided river. *Hydrological Processes*, *31*(4), 756–767. https://doi.org/10.1002/hyp.11033

IRD. (2019). SO HYBAM—The environmental research observatory on the rivers of the Amazon, Orinoco and Congo Basins. Retrieved November 20, 2017, from http://www.ore-hybam.org/

Jarihani, A. A., Callow, J. N., Johansen, K., & Gouweleeuw, B. (2013). Evaluation of multiple satellite altimetry data for studying inland water bodies and river floods. *Journal of Hydrology*, *505*, 78–90. https://doi.org/10.1016/j.jhydrol.2013.09.010

Kim, D., Yu, H., Lee, H., Beighley, E., Durand, M., Alsdorf, D. E., & Hwang, E. (2019). Ensemble learning regression for estimating river discharges using satellite altimetry data: Central Congo River as a Test-bed. *Remote Sensing of Environment*, *221*(2019), 741–755. https://doi.org/10.1016/j.rse.2018.12.010

Laraque, A., Mahe, G., Orange, D., & Marieu, B. (2001). Spatiotemporal variations in hydrological regimes within Central Africa during the XXth century. *Journal of Hydrology*, *245*(1-4), 104–117. https://doi.org/10.1016/S0022-1694(01)00340-7

Lee, H., Beighley, R. E., Alsdorf, D., Jung, H. C., Shum, C. K., Duan, J., et al. (2011). Characterization of terrestrial water dynamics in the Congo Basin using GRACE and satellite radar altimetry. *Remote Sensing of Environment*, *115*(12), 3530–3538. https://doi.org/10.1016/j.rse.2011.08.015

Montazem, A. S., Garambois, P.-A., Calmant, S., Finaud-Guyotm, P., Monnier, J., Moreira, D. M., et al. (2019). Wavelet-based river segmentation using hydraulic control-preserving water surface elevation profile properties. *Geophysical Research Letters*. https://doi.org/10.1029/2019GL082986

Neal, J., Schumann, G., & Bates, P. (2012). A subgrid channel model for simulating river hydraulics and floodplain inundation over large and data sparse areas. *Water Resources Research*, *48*, W11506. https://doi.org/10.1029/2012WR012514

Normandin, C., Frappart, F., Diepkilé, A. T., Marieu, V., Mougin, E., Blarel, F., et al. (2018). Evolution of the performances of radar altimetry missions from ERS-2 to Sentinel-3A over the Inner Niger Delta. *Remote Sensing*, *10*, 833. https://doi.org/10.3390/rs10060833

O'Loughlin, F., Neal, J., Yamazaki, D., & Bates, P. D. (2016). ICESat-derived inland water surface spot heights. *Water Resources Research*, *52*, 3276–3284. https://doi.org/10.1002/2015WR018237

O'Loughlin, F., Trigg, M. A., Schumann, G. J. P., & Bates, P. D. (2013). Hydraulic characterization of the middle reach of the Congo River. *Water Resources Research*, *49*, 5059–5070. https://doi.org/10.1002/wrcr.20398

Pekel, J.-F., Cottam, A., Gorelick, N., & Belward, A. S. (2016). High-resolution mapping of global surface water and its long-term changes. *Nature*, *540*(7633), 418–422. https://doi.org/10.1038/nature20584

Richey, J. E., Melack, J. M., Aufdenkampe, A. K., Ballester, V. M., & Hess, L. L. (2002). Outgassing from Amazonian rivers and wetlands as a large tropical source of atmospheric CO 2. *Nature*, *416*(6881), 617–620. https://doi.org/10.1038/416617a

Robert, M. (1946). *Le Congo physique*. H. Vaillant-Carmanne.

Santos da Silva, J., Calmant, S., Seyler, F., Rotunno Filho, O. C., Cochonneau, G., & Mansur, W. J. (2010). Water levels in the Amazon basin derived from the ERS 2 and ENVISAT radar altimetry missions. *Remote Sensing of Environment*, *114*(10), 2160–2181. https://doi.org/10.1016/j.rse.2010.04.020

Schneider, R., Ridler, M. E., Godiksen, P. N., Madsen, H., & Bauer-Gottwein, P. (2018). A data assimilation system combining CryoSat-2 data and hydrodynamic river models. *Journal of Hydrology*, *557*, 197–210. https://doi.org/10.1016/j.jhydrol.2017.11.052

Trigg, M. A., Wilson, M. D., Bates, P. D., Horritt, M. S., Alsdorf, D. E., Forsberg, B. R., & Vega, M. C. (2009). Amazon flood wave hydraulics. *Journal of Hydrology*, *374*(1–2), 92–105. https://doi.org/10.1016/j.jhydrol.2009.06.004

Trimble. (2019). Trimble centerpoint RTX positioning service. Retrieved February 12, 2019, from https://www.trimble.com/Positioning-Services/CenterPoint-RTX.aspx

Tshimanga, R. M., & Hughes, D. A. (2014). Basin-scale performance of a semidistributed rainfall-runoff model for hydrological predictions and water resources assessment of large rivers: The Congo River. *Water Resources Research*, *50*, 1174–1188. https://doi.org/10.1002/2013WR014310

Urban, T. J., Schutz, B. E., & Neuenschwander, A. L. (2008). A Survey of ICESat coastal altimetry applications: Continental coast, open ocean island, and inland river. *Terrestrial, Atmospheric and Oceanic Sciences*, *19*(1), 1–19. https://doi.org/10.3319/TAO.2008.19.1-2.1(sa)

Yamazaki, D., Ikeshima, D., Tawatari, R., Yamaguchi, T., O'Loughlin, F., Neal, J. C., et al. (2017). A high-accuracy map of global terrain elevations. *Geophysical Research Letters*, *44*, 5844–5853. https://doi.org/10.1002/2017GL072874

Zwally, H., Schutz, R., Bentley, C., Bufton, J., Herring, T., Minster, J., et al. (2012). GLAS/ICESat L2 Antarctic and Greenland Ice Sheet Altimetry Data, Version 33, [GLA14]. Boulder, Colorado USA: NASA DAAC at the National Snow and Ice Data Center